A Novel Individual Variable Step-Size Subband Adaptive Filter Algorithm Robust to Impulsive Noises

TAESU PARK[ID], **MINHO LEE**[ID], **AND POOGYEON PARK**[ID], **(Senior Member, IEEE)**
Department of Electrical Engineering, Pohang University of Science and Technology, Hyoja-dong, Nam-gu, Pohang, Kyungbuk 790-784, South Korea
Corresponding author: PooGyeon Park (ppg@postech.ac.kr)

ABSTRACT This paper proposes a novel individual variable step-size subband adaptive filter algorithm robust to impulsive noises. A fixed step-size subband adaptive filter algorithm that is robust against impulsive noises is newly derived by obtaining the optimal solution from a constrained optimization problem through the Lagrange multiplier. In addition, in order to further improve the convergence performance of the proposed algorithm, the weight update formula with a single fixed step size is modified to have multiple individual step sizes. By analyzing its mean-square-deviation (MSD), the optimal individual step size is designed. Simulation results show that the proposed algorithm outperforms the algorithms robust to impulsive noises in the literature.

INDEX TERMS Adaptive filters, subband adaptive filter algorithm (SAF), variable step size, individual step size, mean square deviation, impulsive noises.

I. INTRODUCTION

Adaptive filters are used in various fields of signal processing such as acoustic echo cancellation, active noise cancellation, channel equalization, and system identification [1]–[5]. They are also used in artificial intelligence and linear algebra recently [6]. Among various adaptive filter algorithms, the least-mean-square (LMS) algorithm and the normalized-least-mean-square (NLMS) algorithm are most used because of their simple structure and good performance [7]–[11]. However, in an environment where the input signal is colored, the convergence speed of the LMS-series algorithms decreases and the steady-state error increases. A normalized-subband-adaptive-filter (NSAF) algorithm was proposed to overcome these shortcomings of the LMS-based algorithms [3], [12]–[17]. Because the NSAF algorithm decomposes and decimates the input and the desired signals for each frequency band, each input signal has the effect of being decorrelated. However, when using a fixed step size in NSAF, there is a trade off between convergence speed and steady state error. Various variable step-size algorithms have

been developed to ensure both fast convergence speed and low steady state error [18]–[24].

In practice, in many cases, the performance of the adaptive filter is degraded due to various measurement noises. In particular, when impulsive noises are included in measurement noises, the performance of VSS NSAFs based on $\mathcal{L}_2$-norm optimization is greatly degraded, and in severe cases, they may diverge. Many studies have been conducted to improve the performance degradation caused by these impulsive noises [25]–[28], [28]–[30]. A sign subband adaptive filter (SSAF) was proposed by minimizing the $\mathcal{L}_1$-norm of a posteriori error, and a variable regularization parameter sign subband adaptive filter (VRP-SSAF) was proposed to improve convergence performance [26]. Subsequently, variable step-size algorithms were developed to improve convergence performance. A variable step-size NSAF algorithm (VSS-SSAF) induced a variable step-size from the viewpoint of minimizing mean square deviation (MSD), but tracking performance was poor [27]. A variable individual step-size NSAF (VISS-NSAF) algorithm individually updates the step size for each subband to improve the convergence performance [23]. A band-dependent variable step-size SSAF algorithm (BDVSS-SSAF) further improved

the convergence performance by applying the individual step size for each subband based on the MSD [28]. A novel SSAF improved performance by applying individual weighting factors to SSAF [31], and a robust band-dependent variable step-size NSAF algorithm (RBDVSS-NSAF) proposed a robust algorithm regardless of the presence of impulsive noise by simultaneously applying $\mathcal{L}_1$ and $\mathcal{L}_2$ optimizations to each subband [30]. These algorithms applying an individual step-size for each subband assume that the divided signals are completely uncorrelated with each other. However, such divided signals are not actually completely uncorrelated with each other, and the correlation among these signals must be considered.

This paper proposes a new individual variable step-size subband algorithm that is robust to impulsive noises. A fixed step-size subband adaptive filter algorithm that is robust against impulsive noises is newly derived by obtaining the optimal solution from a constrained optimization problem through the Lagrange multiplier. The new weight update formula obtained in this way has the effect of normalizing the error signal, so it is naturally robust against impulsive noises. In addition, the correlation among the divided signals for each subband is also considered without any assumptions. Also, the weight update formula with a single fixed step size is modified to have multiple individual step sizes and thereafter the optimal individual step size is obtained through MSD analysis. The proposed algorithm is simulated in the system identification scenario and compared with the existing SAF algorithms that are robust to impulsive noises.

This paper is organized as follows. The NSAF algorithm is briefly mentioned in Section 2. In Section 3, the proposed algorithm robust against impulsive noise is derived, and the individual variable step size is also derived. In Section 4, several simulations are performed while comparing the proposed algorithm with other impulsive noise-resistant algorithms.

II. SUBBAND ADAPTRIVE FILTER ALGORITHM ROBUST TO IMPULSIVE NOISES

A. CONVENTIONAL NORMALIZED SUBBAND ADAPTIVE FILTER ALGORITHM

In conventional NSAF, the desired signal d_n is defined as

$$d_n = \mathbf{x}_n^T \mathbf{w} + v_n. \tag{1}$$

$\mathbf{x}_n$ is the input signal of the NSAF algorithm and its dimension is M. $\mathbf{w}$ is an unknown M-dimensional optimal weight vector. The signal v_n indicates measurement noise with variance σ_v^2. Figure. 1 shows a basic signal flow diagram of NSAF. In the figure, N represents the number of subbands. $\mathbf{H}_j(z)$ is an analysis filter bank that decomposes the signal by frequency band, and $\mathbf{G}_j(z)$ is a synthesis filter bank that reconstructs the divided signal, where $j = 0, 1, \ldots, N-1$. The input signal $\mathbf{x}_n$ and the desired signal d_n are decomposed to frequency bands by the analysis filter bank to become $\mathbf{x}_{j,n}$ and $\mathbf{d}_{j,n}$, respectively. $\mathbf{d}_{j,n}$ is also downsampled by factor N to output $\mathbf{d}_{D,j,k}$. $\mathbf{x}_{j,n}$ is also downsampled by factor N to output $\mathbf{x}_{j,k}$. Then the downsampled signal $\mathbf{x}_{j,k}$ is accumulated N times and
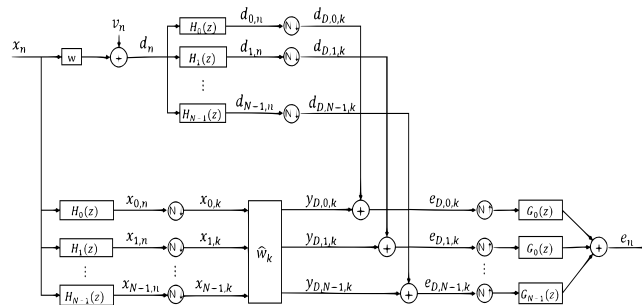

FIGURE 1. The structure of the basic NSAF.

then filtered by an adaptive filter. Therefore, the decimated output signal is defined as $y_{D,j,k} = \mathbf{x}_{j,k}^T \hat{\mathbf{w}}_k$, where $\mathbf{x}_{j,k} = [x_{j,kN}, x_{j,kN-1}, \ldots, x_{j,kN-M+1}]^T$, and $\hat{\mathbf{w}}_k \in \mathcal{R}^{M \times 1}$ is the estimation of the weight coefficient $\mathbf{w}$ at the k-th iteration of the adaptive filter. The decimated desired signal $\mathbf{d}_{D,j,k}$ and $y_{D,j,k}$ are added together. The added signal is then upsampled back to factor N and reconstructed by the synthesis filter bank. In this paper, n represents the iteration of the original signal and k represents the iteration of the downsampling signal. The input matrix, divided output signal, *a priori* error signal, and *a posteriori* error signal are defined as follows:

$$\mathbf{d}_{D,k} = \mathbf{X}_k^T \mathbf{w} + \mathbf{v}_{D,k}, \tag{2}$$

$$\mathbf{e}_{D,k} = \mathbf{d}_{D,k} - \mathbf{X}_k^T \hat{\mathbf{w}}_k, \tag{3}$$

$$\mathbf{e}_{p,k} = \mathbf{d}_{D,k} - \mathbf{X}_k^T \hat{\mathbf{w}}_{k+1}, \tag{4}$$

where $\mathbf{X}_k = [\mathbf{x}_{0,k}, \mathbf{x}_{1,k}, \ldots, \mathbf{x}_{N-1,k}]$ and $\mathbf{v}_{D,k}$ is the measurement noise signal which is divided into frequency bands by the analysis filter bank. In (2), since $\mathbf{X}_k$ and $\mathbf{v}_{D,k}$ are the signals divided into frequency band by analysis filter bank $\mathbf{H}(z)$, each element of $\mathbf{d}_{D,k}$ is a desired signal divided into frequency band. Then, NSAF's weight update recursion formula is as follows.

$$\hat{\mathbf{w}}_{k+1} = \hat{\mathbf{w}}_k + \mu \sum_{j=0}^{N-1} \frac{\mathbf{x}_{j,k}}{\mathbf{x}_{j,k}^T \mathbf{x}_{j,k}} e_{D,j,k}. \tag{5}$$

B. PROPOSED SAF ALGORITHM ROBUST TO IMPULSIVE NOISES

The following constrained optimization problem is set up to obtain a weight update formula that is robust to the impulsive noises.

$$\hat{\mathbf{w}}_k \triangleq \arg\min_{\hat{\mathbf{w}}_k} \mathbf{e}_{p,k}^T \left(\mathbf{X}_k^T \mathbf{X}_k \right)^{-1} \mathbf{e}_{p,k} \tag{6}$$

$$\text{subject to } \| \hat{\mathbf{w}}_{k+1} - \hat{\mathbf{w}}_k \|_2^2 = \mu^2, \tag{7}$$

where μ is a step size that limits the abrupt change in weight vector and is designed in section 3. In order to solve this constrained optimization problem, the Lagrange multiplier λ is introduced as follows:

$$\hat{\mathbf{w}}_{k+1} \triangleq \arg\min_{\hat{\mathbf{w}}_{k+1}} \max_{\lambda} f\left(\hat{\mathbf{w}}_{k+1}, \lambda\right), \tag{8}$$

where the cost function $f\left(\hat{\mathbf{w}}_{k+1}, \lambda\right)$ is described as

$$f\left(\hat{\mathbf{w}}_{k+1}, \lambda\right) \triangleq \mathbf{e}_{p,k}^T \left(\mathbf{X}_k^T \mathbf{X}_k\right)^{-1} \mathbf{e}_{p,k} \\ + \lambda \left(\| \hat{\mathbf{w}}_{k+1} - \hat{\mathbf{w}}_k \|_2^2 - \mu^2\right). \quad (9)$$

The following equation can be obtained by differentiating the cost function of (9) with respect to $\hat{\mathbf{w}}_{k+1}$.

$$\frac{\partial}{\partial \hat{\mathbf{w}}_{k+1}} f\left(\hat{\mathbf{w}}_{k+1}, \lambda\right) \\ = -2\mathbf{X}_k \left(\mathbf{X}_k^T \mathbf{X}_k\right)^{-1} \mathbf{e}_{p,k} + 2\lambda \left(\hat{\mathbf{w}}_{k+1} - \hat{\mathbf{w}}_k\right). \quad (10)$$

If (10) is set to 0 and arranged, the following weight update recursion formula can be obtained.

$$\hat{\mathbf{w}}_{k+1} = \hat{\mathbf{w}}_k + \frac{1}{\lambda} \mathbf{X}_k \left(\mathbf{X}_k^T \mathbf{X}_k\right)^{-1} \mathbf{e}_{p,k}. \quad (11)$$

Similarly, if (9) is partially differentiated with respect to λ and the result is set to 0, we get:

$$\| \hat{\mathbf{w}}_{k+1} - \hat{\mathbf{w}}_k \|_2^2 = \mu^2. \quad (12)$$

Substituting (11) into (12), we get:

$$\frac{1}{\lambda^2} \left(\mathbf{X}_k \left(\mathbf{X}_k^T \mathbf{X}_k\right)^{-1} \mathbf{e}_{p,k}\right)^T \times \left(\mathbf{X}_k \left(\mathbf{X}_k^T \mathbf{X}_k\right)^{-1} \mathbf{e}_{p,k}\right) \\ = \frac{1}{\lambda^2} \mathbf{e}_{p,k}^T \left(\mathbf{X}_k^T \mathbf{X}_k\right)^{-1} \mathbf{e}_{p,k} = \mu^2. \quad (13)$$

Therefore, λ can be represented as

$$\frac{1}{\lambda} = \frac{\mu}{\sqrt{\mathbf{e}_{p,k}^T \left(\mathbf{X}_k^T \mathbf{X}_k\right)^{-1} \mathbf{e}_{p,k}}}. \quad (14)$$

As defined in (4), since the *a posteriori* error $\mathbf{e}_{p,k}$ is a value related to $\hat{\mathbf{w}}_{k+1}$ that is not accessible at the present time, it is reasonable to approximate $\mathbf{e}_{p,k}$ to $\mathbf{e}_{D,k}$. So (11) can be written as follows:

$$\hat{\mathbf{w}}_{k+1} = \hat{\mathbf{w}}_k + \mu \frac{\mathbf{X}_k \left(\mathbf{X}_k^T \mathbf{X}_k\right)^{-1} \mathbf{e}_{D,k}}{\sqrt{\mathbf{e}_{D,k}^T \left(\mathbf{X}_k^T \mathbf{X}_k\right)^{-1} \mathbf{e}_{D,k}}}. \quad (15)$$

III. INDIVIDUAL VARIABLE STEP SIZE
A. ALGORITHM DEVELOPMENT

To develop a individual variable step-size SAF algorithm, the shape of the step size should be modified. We modify the scalar step size into a diagonal matrix form as follows so that different step sizes can be applied to each subband.

$$\hat{\mathbf{w}}_{k+1} = \hat{\mathbf{w}}_k + \frac{\mathbf{X}_k \left(\mathbf{X}_k^T \mathbf{X}_k\right)^{-1} \mathbf{D}_{\mu,k} \mathbf{e}_{D,k}}{\sqrt{\mathbf{e}_{D,k}^T \left(\mathbf{X}_k^T \mathbf{X}_k\right)^{-1} \mathbf{e}_{D,k}}}, \quad (16)$$

where $\mathbf{D}_{\mu,k} = diag[\mu_{0,k}, \mu_{1,k}, \cdots, \mu_{N-1,k}]$. The weight-error vector is defined as $\tilde{\mathbf{w}}_k = \mathbf{w} - \hat{\mathbf{w}}_k$, then (16) can be represented as

$$\tilde{\mathbf{w}}_{k+1} = \tilde{\mathbf{w}}_k - \frac{\mathbf{X}_k \left(\mathbf{X}_k^T \mathbf{X}_k\right)^{-1} \mathbf{D}_{\mu,k} \mathbf{e}_{D,k}}{\sqrt{\mathbf{e}_{D,k}^T \left(\mathbf{X}_k^T \mathbf{X}_k\right)^{-1} \mathbf{e}_{D,k}}}. \quad (17)$$

Since the input matrix $\mathbf{X}_k$ is an observable signal, it is regarded as a deterministic quantity. To perform the MSD analysis, the MSD is defined as $MSD_k \triangleq E\left(\tilde{\mathbf{w}}_k^T \tilde{\mathbf{w}}_k \mid \mathcal{X}_k\right) = Tr\left(\mathbf{P}_k\right)$, where $\mathbf{P}_k \triangleq E\left(\tilde{\mathbf{w}}_k \tilde{\mathbf{w}}_k^T \mid \mathcal{X}_k\right)$ and $\mathcal{X}_k \triangleq \{\mathbf{x}_i \mid 0 \leq i < k\}$. Therefore, the MSD update equation can be expressed as

$$\mathbf{P}_{k+1} = \mathbf{P}_k - 2\mathbb{E}\left[\frac{\mathbf{X}_k \left(\mathbf{X}_k^T \mathbf{X}_k\right)^{-1} \mathbf{D}_{\mu,k} \mathbf{e}_{D,k} \tilde{\mathbf{w}}_k^T}{\sqrt{\mathbf{e}_{D,k}^T \left(\mathbf{X}_k^T \mathbf{X}_k\right)^{-1} \mathbf{e}_{D,k}}}\right] \\ + \mathbb{E}\left[\frac{\mathbf{e}_{D,k}^T \mathbf{D}_{\mu,k} \left(\mathbf{X}_k^T \mathbf{X}_k\right)^{-1} \mathbf{D}_{\mu,k} \mathbf{e}_{D,k}}{\mathbf{e}_{D,k}^T \left(\mathbf{X}_k^T \mathbf{X}_k\right)^{-1} \mathbf{e}_{D,k}}\right]. \quad (18)$$

Since $\tilde{\mathbf{w}}_k$ and $\mathbf{v}_{D,k}$ are assumed to be independent, the second term of (18) can be rearranged as follows:

$$\mathbb{E}\left[\frac{\mathbf{X}_k \left(\mathbf{X}_k^T \mathbf{X}_k\right)^{-1} \mathbf{D}_{\mu,k} \mathbf{e}_{D,k} \tilde{\mathbf{w}}_k^T}{\sqrt{\mathbf{e}_{D,k}^T \left(\mathbf{X}_k^T \mathbf{X}_k\right)^{-1} \mathbf{e}_{D,k}}}\right] \\ \approx \mathbb{E}\left[\frac{\mathbf{X}_k \left(\mathbf{X}_k^T \mathbf{X}_k\right)^{-1} \mathbf{D}_{\mu,k} \mathbf{X}_k^T}{\sqrt{\mathbf{e}_{D,k}^T \left(\mathbf{X}_k^T \mathbf{X}_k\right)^{-1} \mathbf{e}_{D,k}}}\right] \mathbf{P}_k. \quad (19)$$

Also, we define $\mathbf{z}_k$ and $\mathbf{D}_{\mathbf{e}_{D,k}}$ as follows:

$$\mathbf{z}_k^T \triangleq \left[\mu_{0,k} \, \mu_{1,k} \, \cdots \, \mu_{N-1,k}\right], \quad (20)$$
$$\mathbf{D}_{\mathbf{e}_{D,k}} \triangleq diag[e_{D,0,k} \, e_{D,1,k} \, \cdots \, e_{D,N-1,k}]. \quad (21)$$

Then the third term in (18) can be rearranged as follows:

$$\mathbb{E}\left[\frac{\mathbf{e}_{D,k}^T \mathbf{D}_{\mu,k} \left(\mathbf{X}_k^T \mathbf{X}_k\right)^{-1} \mathbf{D}_{\mu,k} \mathbf{e}_{D,k}}{\mathbf{e}_{D,k}^T \left(\mathbf{X}_k^T \mathbf{X}_k\right)^{-1} \mathbf{e}_{D,k}}\right] \\ = \mathbb{E}\left[\frac{\mathbf{z}_k^T \mathbf{D}_{\mathbf{e}_{D,k}} \left(\mathbf{X}_k^T \mathbf{X}_k\right)^{-1} \mathbf{D}_{\mathbf{e}_{D,k}}^T \mathbf{z}_k}{\mathbf{e}_{D,k}^T \left(\mathbf{X}_k^T \mathbf{X}_k\right)^{-1} \mathbf{e}_{D,k}}\right]. \quad (22)$$

Therefore, (18) is finally summarized as follows.

$$\mathbf{P}_{k+1} \approx \mathbf{P}_k - 2\mathbb{E}\left[\frac{\mathbf{X}_k \left(\mathbf{X}_k^T \mathbf{X}_k\right)^{-1} \mathbf{D}_{\mu,k} \mathbf{X}_k^T}{\sqrt{\mathbf{e}_{D,k}^T \left(\mathbf{X}_k^T \mathbf{X}_k\right)^{-1} \mathbf{e}_{D,k}}}\right] \mathbf{P}_k \\ + \mathbf{z}_k^T \mathbb{E}\left[\frac{\mathbf{D}_{\mathbf{e}_{D,k}} \left(\mathbf{X}_k^T \mathbf{X}_k\right)^{-1} \mathbf{D}_{\mathbf{e}_{D,k}}^T}{\mathbf{e}_{D,k}^T \left(\mathbf{X}_k^T \mathbf{X}_k\right)^{-1} \mathbf{e}_{D,k}}\right] \mathbf{z}_k. \quad (23)$$

For the convenience of notation, $\rho \triangleq \sqrt{\mathbf{e}_{D,k}^T \left(\mathbf{X}_k^T \mathbf{X}_k\right)^{-1} \mathbf{e}_{D,k}}$, and $\mathbf{A}_k \triangleq \left(\mathbf{D}_{\mathbf{e}_{D,k}} \left(\mathbf{X}_k^T \mathbf{X}_k\right)^{-1} \mathbf{D}_{\mathbf{e}_{D,k}}^T\right) / \left(\mathbf{e}_{D,k}^T \left(\mathbf{X}_k^T \mathbf{X}_k\right)^{-1} \mathbf{e}_{D,k}\right)$ are defined. After that, taking traces on both side of (23) and using the same approximation method as in [32], [33], the following approximation can be obtained.

$$p_{k+1} \approx p_k - 2\frac{Np_k}{\rho \beta M} \mathbf{l}_N^T \mathbf{z}_k + \mathbf{z}_k^T \mathbb{E}\left[\mathbf{A}_k\right] \mathbf{z}_k, \quad (24)$$

where $\mathbf{l}_N$ is a $N \times 1$ vector which components are all 1 and β is a design parameter that the user optimizes according to

the environment. By differentiating p_{k+1} with respect to $\mathbf{z}_k$ to minimize MSD, the following equation can be obtained:

$$\frac{Np_k}{\rho\beta M}\mathbf{1}_N = \mathbb{E}[\mathbf{A}_k]\mathbf{z}_k. \quad (25)$$

Therefore, the optimal $\mathbf{z}_k$ can be obtained as follows.

$$\mathbf{z}_k = \mathbb{E}^{-1}[\mathbf{A}_k]\frac{Np_k}{\rho\beta M}\mathbf{1}_N. \quad (26)$$

According to the definition of $\mathbf{A}_k$, the following expression holds.

$$\mathbb{E}[\mathbf{A}_k] = \mathbb{E}\left[\frac{\mathbf{D}_{\mathbf{e}_{D,k}}\left(\mathbf{X}_k^T\mathbf{X}_k\right)^{-1}\mathbf{D}_{\mathbf{e}_{D,k}}^T}{\mathbf{e}_{D,k}^T\left(\mathbf{X}_k^T\mathbf{X}_k\right)^{-1}\mathbf{e}_{D,k}}\right]. \quad (27)$$

Based on this fact, we use the estimate of $\mathbf{A}_k$, which is $\hat{\mathbf{A}}_k$, as follows through the moving average method.

$$\hat{\mathbf{A}}_k = \alpha\hat{\mathbf{A}}_{k-1} + (1-\alpha)\frac{\mathbf{D}_{\mathbf{e}_{D,k}}\left(\mathbf{X}_k^T\mathbf{X}_k\right)^{-1}\mathbf{D}_{\mathbf{e}_{D,k}}^T}{\mathbf{e}_{D,k}^T\left(\mathbf{X}_k^T\mathbf{X}_k\right)^{-1}\mathbf{e}_{D,k}}, \quad (28)$$

where α is the forgetting factor with a value between 0 and 1. Therefore, the final weight update formula can be written as follows:

$$\hat{\mathbf{w}}_{k+1} = \hat{\mathbf{w}}_k + \frac{\mathbf{X}_k\left(\mathbf{X}_k^T\mathbf{X}_k\right)^{-1}\mathbf{D}_{\mu,k}\mathbf{e}_{D,k}}{\sqrt{\mathbf{e}_{D,k}^T\left(\mathbf{X}_k^T\mathbf{X}_k\right)^{-1}\mathbf{e}_{D,k}}}. \quad (29)$$

$\mathbf{z}_k$ represents the step size for each subband in the form of a vector. Therefore, the i th diagonal element of $\mathbf{D}_{\mu,k}$ is the i th element of $\mathbf{z}_k$. Since the proposed algorithm is developed in a stationary environment, a method is needed to make the algorithm work well even when an unknown system suddenly changes. For this reset method, the method used in [28] is applied. This is summarized in table 1.

B. STABILITY
In order to find the range of the step size in which the stability of the algorithm is guaranteed, (24) is summarized as follows.

$$p_{k+1} \approx p_k - 2\frac{Np_k}{\rho\beta M}\mathbf{1}_N^T\mathbf{z}_k + \mathbf{z}_k^T\mathbb{E}[\mathbf{A}_k]\mathbf{z}_k$$
$$= \left(1 - 2\frac{N}{\rho\beta M}\mathbf{1}_N^T\mathbf{z}_k\right)p_k + \mathbf{z}_k^T\mathbb{E}[\mathbf{A}_k]\mathbf{z}_k. \quad (30)$$

In order to guarantee the convergence of the proposed algorithm, the following conditions must be satisfied.

$$\left|1 - 2\frac{N}{\rho\beta M}\mathbf{1}_N^T\mathbf{z}_k\right| < 1. \quad (31)$$

According to the definitions of ρ and $\mathbf{z}_k$, (31) is arranged as follows.

$$0 < \frac{N\sum_{j=0}^{N-1}\mu_{j,k}}{\beta M\sqrt{\mathbf{e}_{D,k}^T\left(\mathbf{X}_k^T\mathbf{X}_k\right)^{-1}\mathbf{e}_{D,k}}} < 1. \quad (32)$$

TABLE 1. Proposed algorithm summary.

1. Initialization.

$$\hat{\mathbf{w}}_0 = 0, \mathbf{D}_{\mu,0} = \mathbf{I}_N, \mathbf{z}_0 = \mathbf{1}_N, \hat{\mathbf{A}}_0 = \mathbf{I}_N, p_0 = 1,$$
$$V_1 = M,, V_2 = 0.75V_1, \zeta = 1, \epsilon = 10^{-6}.$$

2. Parameters.

$$\beta = 30, \alpha = 0.999$$

3. Adaptation.

$$\hat{\mathbf{A}}_k = \alpha\hat{\mathbf{A}}_{k-1} + (1-\alpha)\frac{\mathbf{D}_{\mathbf{e}_{D,k}}\left(\mathbf{X}_k^T\mathbf{X}_k\right)^{-1}\mathbf{D}_{\mathbf{e}_{D,k}}^T}{\mathbf{e}_{D,k}^T\left(\mathbf{X}_k^T\mathbf{X}_k\right)^{-1}\mathbf{e}_{D,k}}$$
$$\mathbf{z}_k = \hat{\mathbf{A}}_k\frac{Np_k}{\rho\beta M}\mathbf{1}_N$$
$$\hat{\mathbf{w}}_{k+1} = \hat{\mathbf{w}}_k + \frac{\mathbf{X}_k\left(\mathbf{X}_k^T\mathbf{X}_k\right)^{-1}\mathbf{D}_{\mu,k}\mathbf{e}_{D,k}}{\sqrt{\mathbf{e}_{D,k}^T\left(\mathbf{X}_k^T\mathbf{X}_k\right)^{-1}\mathbf{e}_{D,k}}},$$
where the i-th diagonal element of $\mathbf{D}_{\mu,k}$ is the i-th element of $\mathbf{z}_k$.

4. Reset method.

  if $mod(k, V_1/N) = 0$

$$\mathbf{Q} = sort\left(\frac{|e(k-1)|}{\|\mathbf{x}_k\|_2+\epsilon}, ..., \frac{|e(k-1)|}{\|\mathbf{x}_{k-V_1+1}\|_2+\epsilon}\right)^T$$
$$ctrl_{new} = \frac{\mathbf{Q}^T\mathbf{R}\mathbf{Q}^T}{V_1-V_2}$$

  end
  if $\frac{ctrl_{new}-ctrl_{old}}{\frac{1}{N}\mathbf{1}_N^T\mathbf{z}_k/N} > \zeta$

$$\mathbf{z}_k = \mathbf{1}_N, \hat{\mathbf{A}}_k = \mathbf{I}_N, p_{k=1}$$

  else *proposed NIVSS − NSAF's update*
  end
  where $\mathbf{R}$ is a diagonal matrix in which the first $V_1 - V_2$ elements are 1 and the rest are 0.

Therefore, the condition for step sizes that guarantee the stability of the algorithm is as follows.

$$0 < \sum_{j=0}^{N-1}\mu_{j,k} < \frac{\beta M\sqrt{\mathbf{e}_{D,k}^T\left(\mathbf{X}_k^T\mathbf{X}_k\right)^{-1}\mathbf{e}_{D,k}}}{N}. \quad (33)$$

IV. SIMULATION RESULTS
We perform computer simulation in this section to verify the performance of the algorithm proposed in the system identification scenario. The filter coefficients of the system identified in the simulation are generated as a random unit vector. In this simulation, the two filter banks $\mathbf{H}(z)$ and $\mathbf{G}(z)$ are designed to be paraunitary so that the signals that have passed through the analysis filter bank and the synthesis filter bank are perfectly reconstructed. That is, analysis filter bank $\mathbf{H}(z)$ and synthesis filter bank $\mathbf{G}(z)$ satisfy the following conditions.

$$\mathbf{H}(z)\mathbf{G}(z) = \mathbf{I}. \quad (34)$$

The autoregressive (AR) models are defined in (35) and (36) to confirm that the proposed algorithm works well not only in white Gaussian input but also in AR input environment. The impulsive noise environment is created with $\eta_i = q_iA_i$. q_i follows the Bernoulli process with a probability of $P[q_i = 1] = Pr$, and A_i is white Gaussian noise with

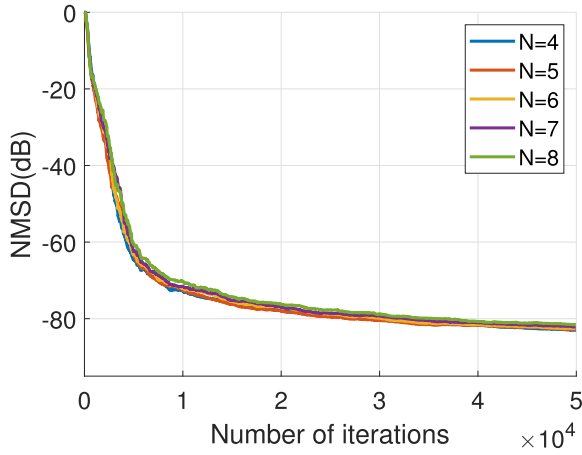**FIGURE 2.** MSD learning curves according to the number of subbands of the proposed algorithm (M = 64, white Gaussian input, Pr = 0).
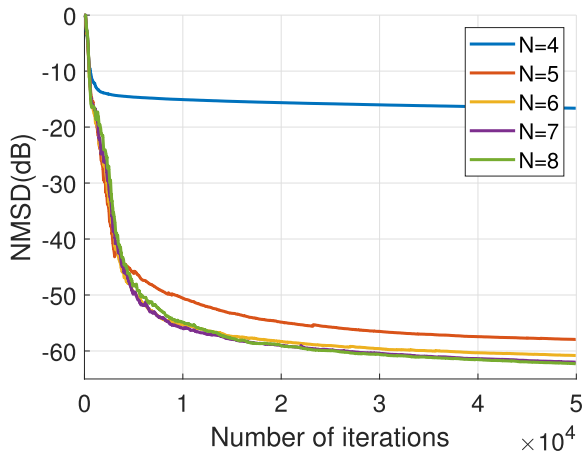

FIGURE 4. Performance comparison between the proposed algorithm and fixed step-size NSAF (M = 64, White Gaussian input, Pr = 0.1).

FIGURE 3. MSD learning curve according to the number of subbands of the proposed algorithm (M = 64, colored by $R_2(z)$, Pr = 0).

FIGURE 5. Performance comparison between the proposed algorithm and existing algorithms that are robust to impulsive noises (M = 64, White Gaussian input, Pr = 0.01).

zero mean. In addition, to show that the performance of the proposed algorithm is not a coincidence, all simulations are obtained through averaging of 10 ensembles.

$$R_1(z) = \frac{1}{1 - 0.97z^{-1}}, \tag{35}$$

$$R_2(z) = \frac{1}{1 - 1.6z^{-1} + 0.81z^{-2}}. \tag{36}$$

A. SELF WHITENING EFFECT ACCORDING TO THE NUMBER OF SUBBANDS

The advantage of subband adaptive filter is that performance degradation is minimized due to self input whitening effect in colored input situation. Therefore, it is important to set the appropriate number of subbands in the colored input situation. The length of the analysis filter was set to 8 times the number of subbands. Figure. 2 shows the MSD learning curves by the number of subbands of the proposed algorithm in a white Gaussian input environment. In such an environment, since the input signal is already white Gaussian, there
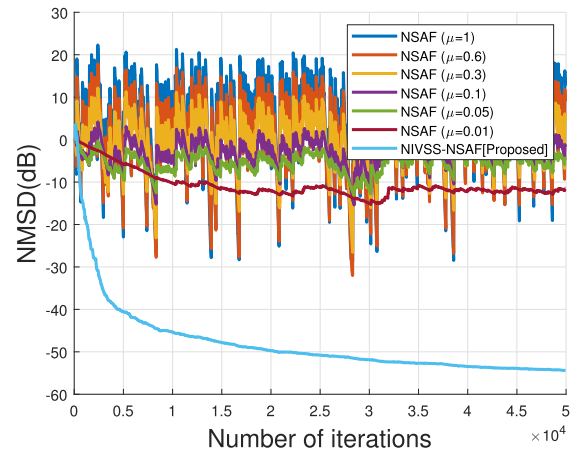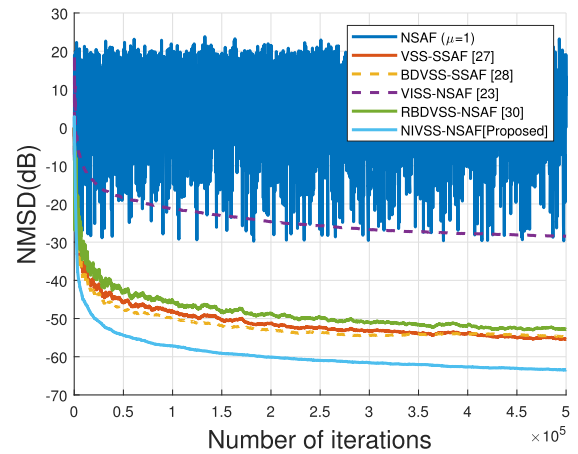
is little difference in MSD learning curves by the number of subbands. Figure. 3 shows the MSD learning curves by the number of subbands of the proposed algorithm in the input signal environment correlated with $R_2(z)$. In such an environment, as the number of subbands increases, the performance degradation due to colored input is alleviated by the self input whitening effect. This self input whitening effect is saturated at N = 8, which means that 8 subbands sufficiently whiten the colored input.

B. SIMULATION OF THE PROPOSED ALGORITHM AND FIXED STEP-SIZE NSAF IN THE ENVIRONMENT OF IMPULSIVE NOISES

Figure. 4 shows the performance comparison of the proposed algorithm and the basic NSAF algorithm in the impulsive noises environment. Simulation environment variables were set to $M = 64$, $N = 8$, $SNR = 30dB$, $SIR = -30dB$, $Pr = 0.1$. As shown in figure. 4, the basic NSAF algorithms using
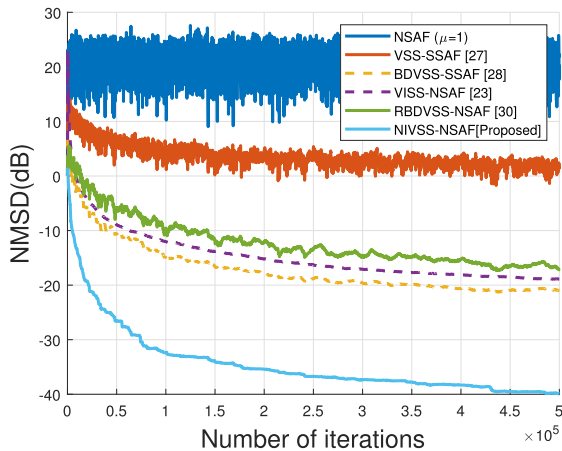
FIGURE 6. Performance comparison between the proposed algorithm and existing algorithms that are robust to impulsive noises (M = 64, White Gaussian input, Pr = 0.1).
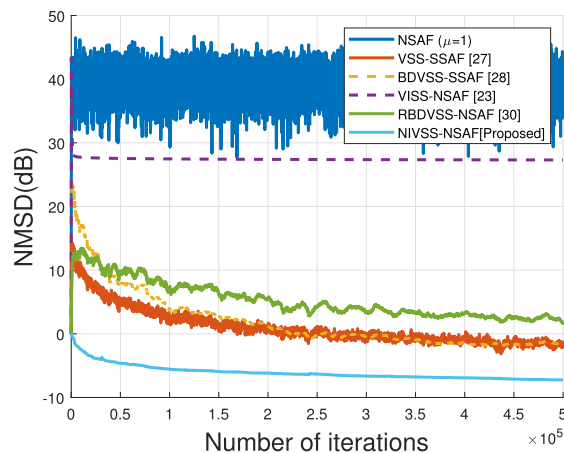
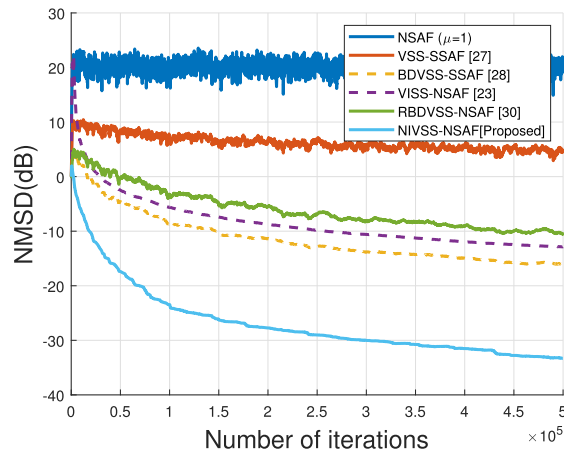

FIGURE 8. Performance comparison between the proposed algorithm and existing algorithms that are robust to impulsive noises (M = 64, AR_2 input, Pr = 0.1).
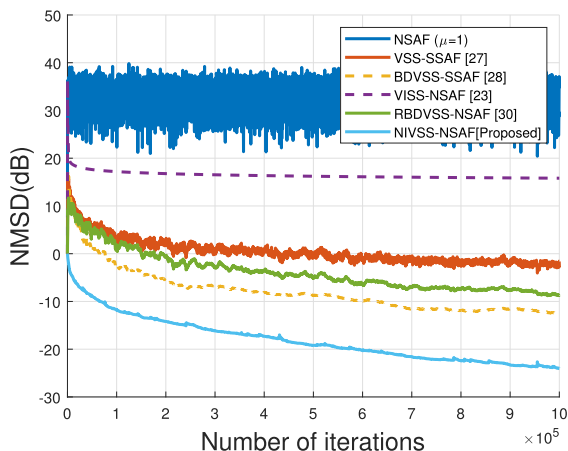
FIGURE 7. Performance comparison between the proposed algorithm and existing algorithms that are robust to impulsive noises (M = 64, AR_1 input, Pr = 0.1).

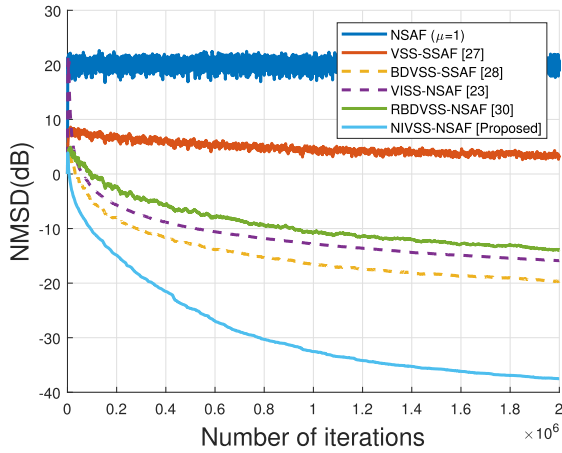

FIGURE 9. Performance comparison between the proposed algorithm and existing algorithms that are robust to impulsive noises (M = 256, White Gaussian input, Pr = 0.1).

a fixed step-size diverge in an impulsive noise environment. As the step size decreases, the influence of the error including impulsive noises decreases, so it seems to be less divergent, but it can be seen that weight update is hardly performed. On the other hand, since the proposed algorithm has the effect of normalizing the error signal, it shows a fast convergence speed and a lower steady state error even in an impulsive noise environment.
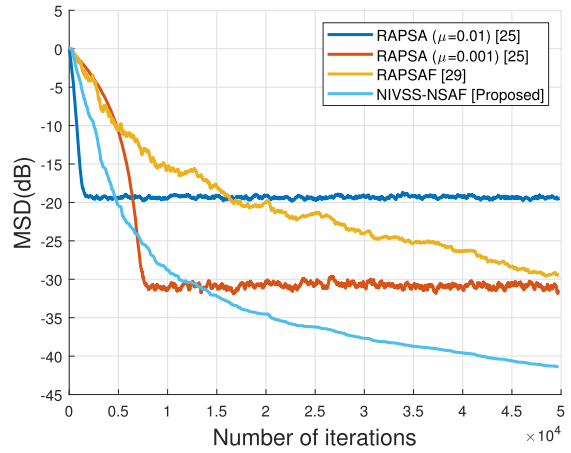
C. PERFORMANCE COMPARISON
Figure. 5-10 show a comparison of the proposed algorithm with algorithms that have good performance robust to impulsive noise. The tuning parameters of the comparison algorithms are set as follows: $\kappa = 5$, $\alpha = 1 - N/\kappa m$ for VSS-SSAF [27], $\lambda = 1 - N/\kappa m$, $C = 1.483 \left(1 + \frac{5}{N_w - 1}\right)$, $V_T = N_w = M$, $V_D = 0.75V_T$, $\xi = 1$, $\epsilon = 10^{-6}$ for BDVSS-SSAF [28], $\beta = 15$, $Tr[\mathbf{P}(0)] = 100$ for VISS-NSAF [23],

$\lambda = 1 - N/\kappa M$, $\kappa = 5$, $V_T = 3M$, $V_D = 0.75V_T$, $\xi_{th} = 1$, $\epsilon = 10^{-6}$ for RBDVSS-NSAF [30]. Figure. 5 and 6 show the performance comparison between the algorithms that are robust against impulsive noises and the proposed algorithm. In both simulations, M = 64, N = 8, SNR = 30dB, SIR = -30dB and input signal is white Gaussian were set. Pr is set to 0.01 in figure. 5, and set to 0.1 in figure. 6. As shown in the simulations, VSS-SSAF is robust in impulsive noises environment because only the sign of the error signal is used as information when updating weights [9]. In addition, a variable step size was applied to improve the convergence performance. VISS-NSAF tried to further improve the convergence performance by applying an individual variable step size for each frequency band, but it is very vulnerable to impulsive noises, so it does not converge well [23]. Since BDVSS-SSAF applies variable step size for each frequency band to SSAF, it is robust against impulsive noises and the convergence performance is further improved [28]. RBDVSS-NSAF also

FIGURE 10. Performance comparison between the proposed algorithm and existing algorithms that are robust to impulsive noises (M = 512, White Gaussian input, Pr = 0.1).

FIGURE 12. Performance comparison between RAPSA, RAPSAF, and proposed NIVSS-NSAF (M = 256, White Gaussian input, Pr = 0.01).
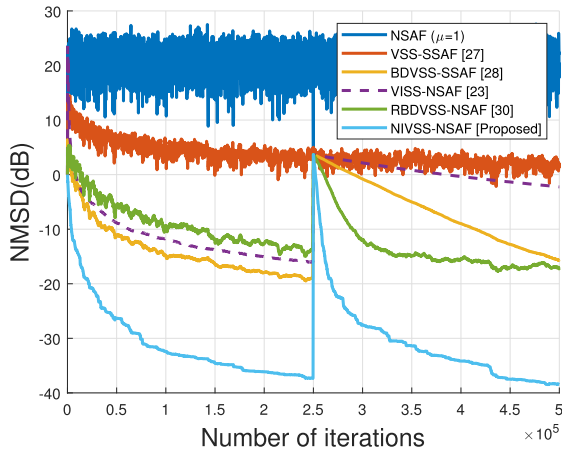
FIGURE 11. Performance comparison between the proposed algorithm and existing algorithms that are robust to impulsive noises in a rapidly changing system environment (M = 256, White Gaussian input, Pr = 0.1).

showed good performance by applying a variable step size for each frequency band to an algorithm that is robust against impulsive noises [30]. However, it was confirmed that the proposed algorithm improved the convergence speed and steady state error more than other algorithms mentioned above through the application of a new weight update method that normalizes the error signal and a new individual variable step size.

Additional simulations are shown in figure. 7-10 to show that the proposed algorithm has good performance for various parameters. Figure. 7 and 8 are simulation results when a white Gaussian signal correlated with $R_1(z)$ and $R_2(z)$, respectively, is used as an input. Other parameters were the same, and Pr was set to 0.1. Simulation results confirm that the NIVSS-NSAF algorithm for colored input signals also has the best performance in impulsive noises environment. Figure. 9 and 10 are simulation results for different tap lengths. In both simulations, the other parameters are the

same as in the previous simulation, and the tap lengths are set to 256 and 512, respectively. The input signal follows the white Gaussian distribution, and the frequency of occurrence of impulsive noises is 0.1. As can be seen from the simulation results, it was confirmed that the proposed NIVSS-NSAF has consistently excellent performance in various tap lengths. Figure. 11 shows the tracking performance of the proposed algorithm and comparison algorithms when the coefficient of an unknown system suddenly changes in the middle of the whole iteration. Even in a situation where the system changes rapidly in the middle, the proposed algorithm estimates the unknown system again by the reset method and shows better performance than other algorithms. Figure. 12 compares the proposed algorithm with the existing RAPSA [25] and RAPSAF [29]. In general, the NSAF algorithm has a lower computational amount than APA, but the proposed algorithm has to calculate all multiple step sizes, so the computational amount is similar to that of APA. As shown in figure. 12, RAPSA uses a fixed step size, so there is still a trade-off between the convergence speed and the steady-state error, but the proposed algorithm shows a sufficiently good convergence performance without such trade-off. In addition, although the RAPSAF algorithm is also a subband affine projection algorithm that is robust against impulsive noises, it can be confirmed that the convergence performance of the proposed algorithm is better than the RAPSAF algorithm as shown in figure. 12.

V. CONCLUSION
This paper proposed the NIVSS-NSAF algorithm that is robust against impulsive noises. An optimal solution of the constrained optimization problem was obtained through the Lagrange multiplier. Since the derived algorithm has the effect of normalizing the error signal, it is robust against impulsive noises. In addition, the individual variable step sizes obtained through the MSD analysis of the proposed algorithm improved not only the convergence speed of the

proposed algorithm, but also the steady state error performance. The simulation results showed that the proposed algorithm in the system identification scenario outperforms other existing variable step-size SAF algorithms robust to impulsive noises.

REFERENCES

[1] A. H. Sayed, *Fundamentals of Adaptive Filtering*. Hoboken, NJ, USA: Wiley, 2003.

[2] S. S. Haykin, *Adaptive Filter Theory*. Chennai, India: Pearson, 2005.

[3] K.-A. Lee, W.-S. Gan, and S. M. Kuo, *Subband Adaptive Filtering: Theory and Implementation*. Hoboken, NJ, USA: Wiley, 2009.

[4] Y. V. Zakharov and J. Li, "Sliding-window homotopy adaptive filter for estimation of sparse UWA channels," in *Proc. IEEE Sensor Array Multichannel Signal Process. Workshop (SAM)*, Jul. 2016, pp. 1–4.

[5] M. Yukawa, R. C. de Lamare, and R. Sampaio-Neto, "Efficient acoustic echo cancellation with reduced-rank adaptive filtering based on selective decimation and adaptive interpolation," *IEEE Trans. Audio, Speech, Language Process.*, vol. 16, no. 4, pp. 696–710, May 2008.

[6] D. W. Kim, M. S. Kim, J. Lee, and P. Park, "Adaptive learning-rate backpropagation neural network algorithm based on the minimization of mean-square deviation for impulsive noises," *IEEE Access*, vol. 8, pp. 98018–98026, 2020.

[7] H.-C. Huang and J. Lee, "A new variable step-size NLMS algorithm and its performance analysis," *IEEE Trans. Signal Process.*, vol. 60, no. 4, pp. 2055–2060, Apr. 2012.

[8] J. Hur, M. Lee, D. Kim, and P. Park, "A variable step-size robust saturation algorithm against impulsive noises," *IEEE Trans. Circuits Syst. II, Exp. Briefs*, vol. 67, no. 10, pp. 2279–2283, Oct. 2020.

[9] L. Shi, H. Zhao, X. Zeng, and Y. Yu, "Variable step-size widely linear complex-valued NLMS algorithm and its performance analysis," *Signal Process.*, vol. 165, pp. 1–6, Dec. 2019.

[10] L. R. Vega, H. Rey, J. Benesty, and S. Tressens, "A new robust variable step-size NLMS algorithm," *IEEE Trans. Signal Process.*, vol. 56, no. 5, pp. 1878–1893, May 2008.

[11] A. I. Sulyman and A. Zerguine, "Convergence and steady-state analysis of a variable step-size NLMS algorithm," *Signal Process.*, vol. 83, no. 6, pp. 1255–1273, Jun. 2003.

[12] S. S. Pradham and V. U. Reddy, "A new approach to subband adaptive filtering," *IEEE Trans. Signal Process.*, vol. 47, no. 3, pp. 655–664, Mar. 1999.

[13] K. A. Lee and W. S. Gan, "Inherent decorrelating and least perturbation properties of the normalized subband adaptive filter," *IEEE Trans. Signal Process.*, vol. 54, no. 11, pp. 4475–4480, Nov. 2006.

[14] K. A. Lee and W. S. Gan, "Improving convergence of the NLMS algorithm using constrained subband updates," *IEEE Signal Process. Lett.*, vol. 11, no. 9, pp. 736–739, Sep. 2004.

[15] W. Yin and A. S. Mehr, "Stochastic analysis of the normalized subband adaptive filter algorithm," *IEEE Trans. Circuits Syst. I, Reg. Papers*, vol. 58, no. 5, pp. 1020–1033, May 2011.

[16] Y. Yu, H. He, B. Chen, J. Li, Y. Zhang, and L. Lu, "M-estimate based normalized subband adaptive filter algorithm: Performance analysis and improvements," *IEEE/ACM Trans. Audio, Speech, Language Process.*, vol. 28, pp. 225–239, 2020.

[17] Y. Yu, T. Yang, H. Chen, R. C. D. Lamare, and Y. Li, "Sparsity-aware SSAF algorithm with individual weighting factors: Performance analysis and improvements in acoustic echo cancellation," *Signal Process.*, vol. 178, Jan. 2021, Art. no. 107806.

[18] J. Ni and F. Li, "A variable step-size matrix normalized subband adaptive filter," *IEEE Trans. Audio, Speech, Language Process.*, vol. 18, no. 6, pp. 1290–1299, Aug. 2010.

[19] Y. Yu, H. Zhao, and B. Chen, "A new normalized subband adaptive filter algorithm with individual variable step sizes," *Circuits, Syst., Signal Process.*, vol. 35, no. 4, pp. 1407–1418, Apr. 2016.

[20] J. J. Jeong, K. Koo, G. T. Choi, and S. W. Kim, "A variable step size for normalized subband adaptive filters," *IEEE Signal Process. Lett.*, vol. 19, no. 12, pp. 906–909, Dec. 2012.

[21] J. Shin, N. Kong, and P. Park, "Normalised subband adaptive filter with variable step size," *Electron. Lett.*, vol. 48, no. 4, pp. 204–206, 2012.

[22] P. Wen and J. Zhang, "A novel variable step-size normalized subband adaptive filter based on mixed error cost function," *Signal Process.*, vol. 138, pp. 48–52, Sep. 2017.

[23] J.-H. Seo and P. Park, "Variable individual step-size subband adaptive filtering algorithm," *Electron. Lett.*, vol. 50, no. 3, pp. 177–178, 2014.

[24] Y. Yu and H. Zhao, "A band-independent variable step size proportionate normalized subband adaptive filter algorithm," *AEU, Int. J. Electron. Commun.*, vol. 70, no. 9, pp. 1179–1186, Sep. 2016.

[25] T. Shao, Y. R. Zheng, and J. Benesty, "An affine projection sign algorithm robust against impulsive interferences," *IEEE Signal Process. Lett.*, vol. 17. no. 4, pp. 327–330, Apr. 2010.

[26] J. Ni and F. Li, "Variable regularisation parameter sign subband adaptive filter," *Electron. Lett.*, vol. 46, no. 24, pp. 1605–1607, 2010.

[27] J. Shin, J. Yoo, and P. Park, "Variable step-size sign subband adaptive filter," *IEEE Signal Process. Lett.*, vol. 20, no. 2, pp. 173–176, Feb. 2013.

[28] J. Yoo, J. Shin, and P. Park, "A band-dependent variable step-size sign subband adaptive filter," *Signal Process.*, vol. 104, pp. 407–411, Nov. 2014.

[29] M. R. Petraglia, E. L. Marques, and D. B. Haddad, "Low-complexity affine projection subband algorithm for robust adaptive filtering in impulsive noise," in *Proc. IEEE Sensor Array Multichannel Signal Process. Workshop (SAM)*, Jul. 2016, pp. 1–5.

[30] Y. Yu, H. Zhao, Z. He, and B. Chen, "A robust band-dependent variable step size NSAF algorithm against impulsive noises," *Signal Process.*, vol. 119, pp. 203–208, Feb. 2016.

[31] Y. Yu and H. Zhao, "Novel sign subband adaptive filter algorithms with individual weighting factors," *Signal Process.*, vol. 122, pp. 14–23, May 2016.

[32] P. Park, M. Chang, and N. Kong, "Scheduled-stepsize NLMS algorithm," *IEEE Signal Process. Lett.*, vol. 16, no. 12, pp. 1055–1058, Dec. 2009.

[33] C. H. Lee and P. Park, "Scheduled-step-size affine projection algorithm," *IEEE Trans. Circuits Syst. I, Reg. Papers*, vol. 59, no. 9, pp. 2034–2043, Sep. 2012.

TAESU PARK received the B.S. degree in electronics engineering from Kyungpook National University, Daegu, South Korea, in 2015, and the M.S. degree in electrical engineering from Pohang University of Science and Technology, Pohang, South Korea, in 2017, where he is currently pursuing the Ph.D. degree. His research interests include signal processing, state estimation, and artificial intelligence.

MINHO LEE received the B.S. degree in electronics engineering from Kyungpook National University, Daegu, South Korea, in 2015, and the M.S. degree in electrical engineering from Pohang University of Science and Technology, Pohang, South Korea, in 2018, where he is currently pursuing the Ph.D. degree. His research interests include signal processing, state estimation, and artificial intelligence.

POOGYEON PARK (Senior Member, IEEE) received the B.S. and M.S. degrees in control and instrumentation engineering from Seoul National University, Seoul, South Korea, in 1988 and 1990, respectively, and the Ph.D. degree from Stanford University, Stanford, CA, USA, in 1995.

From 1996 to 2000, he was an Assistant Professor with Pohang University of Science and Technology. Since 2006, he has been a Professor with the Electronic Electrical Engineering Department, Pohang University of Science and Technology. He has authored over 170 articles and the total citation for his articles is 9712. His research interests include control and signal processing.

• • •